A Topological Analysis of Electron Density in Cation−π Complexes

E. Cubero,[†] M. Orozco,*[,†] and F. J. Luque*[,‡]

Departament de Bioquímica i Biologia Molecular, Facultat de Química, Universitat de Barcelona, Martí i Franqués 1, 08028 Barcelona, Spain, and Departament de Fisicoquímica, Facultat de Farmàcia, Universitat de Barcelona, Av. Diagonal s/n, 08028 Barcelona, Spain

Received: August 17, 1998; In Final Form: October 30, 1998

A topological analysis of the electron density in cation−π complexes is presented. Calculations are performed for complexes involving the interaction of the Na^+ ion with a variety of six- and five-membered aromatic rings, as well as for the interaction of benzene with diverse cations and hydrogen-bonded neutral molecules. The results reveal the existence of great differences in the topological features of the electron density, which reflect the profound influence of the substituents attached to the aromatic core or of the presence of heteroatoms and fused rings. Nevertheless, with exception of the complexes involving five-membered rings, there are strong relationships between the charge density at the cage critical points and both the energetic and geometrical parameters of the complexes. These relationships allow us to generalize the concept of bond order−bond length found for other intermolecular interactions.

Introduction

Cation−π interactions are recognized to be strong noncovalent binding forces with a large importance in a wide range of systems, including small organic molecules, supramolecules and biochemical macromolecules.[1−6] Much of the information on cation−π interactions comes from crystallographic studies, but further support is given by data in the gas phase and in solution.[1,7] Most studies have addressed the nature and energetics of cation−π interactions.[8−15] The results showed that for complexes of simple ions, i.e., Li^+ or Na^+, calculations at the Hartree−Fock level are adequate, but correlation effects can be quantitatively important for complexes involving cations such as $N(CH_3)_4^+$. The cation−π interaction is in general dominated by electrostatic and cation-induced polarization. As we have recently shown,[15] these two terms explain around 99% of the variance in the binding energies for a series of 16 Na^+−π complexes that includes both six- and five-membered aromatic rings.

The aim of this study is to examine the main features of cation−π interactions in terms of the topological properties of the electron charge density. Such an analysis can be done efficiently using the theory of "atoms in molecules".[16,17] This approach has been successfully used to characterize the formation of hydrogen bonds in a variety of molecular complexes.[18−25] Moreover, several studies have shown a clear relationship between the topological properties of the charge density in hydrogen-bonded complexes with both the interaction energy and the internuclear distance of the complexes.[26,27] The theory has been also used for the understanding of the cation complexation to the heteroatom lone electron pairs in heterocycles, like the binding of Li^+ to the nitrogen atom in azoles and azines,[28,29] but to our knowledge it has not yet been used to characterize cation−π interactions.

In this paper we have examined the interaction of Na^+ with a series of derivatives on benzene. Indeed, we have extended such an analysis to the interaction of Na^+ with five-membered aromatic rings, as well as to the interaction of benzene with a variety of chemical systems including both cations and hydrogen-bonded neutral molecules. Particularly, we have investigated the relationship of the topological properties with both the energetics and geometrical features in these complexes. The results evidence the complexity of the cation−π interaction as far as the topology of the electron density is concerned, but they also show the existence of relationships between the topological features and the energetics of cation−π complexes.

Methods

Topological Properties of Electron Density. A brief review of some relevant concepts within Bader's topology analysis is appropriate to facilitate the analysis of the results (the reader is addressed to refs 16 and 17 for a more comprehensive explanation). The existence of a bond path linking two nuclei in an equilibrium structure implies that the two atoms are bonded to one another. Such a path is characterized by the bond critical point, which is the point of minimum charge density along the bond, but a maximum along the directions perpendicular to the bond path. A critical point can be characterized by the number of zero eigenvalues of the associated Hessian matrix, which determines its rank, and the algebraic sum of their signs, which determine its signature. A bond critical point is denoted as (3, −1) and has one positive (λ_3) and two negative (λ_1, λ_2) curvatures, one (λ_3) associated with the charge density along the bond path and the other (λ_1, λ_2) perpendicular to the bond path. An interesting feature is the ellipticity (ϵ), which is defined as $\lambda_1/\lambda_2 - 1$ and gives a measure of the extent to which electron density is accumulated in a given plane. Thus, the ellipticity for a cylindrical symmetrical bond like C−C in ethane is 0.0, and it amounts to around 0.45 for ethene. There can be other types of nondegenerate critical points: (3, −3), (3, +1), and (3, +3). The first corresponds to position of local maxima of the charge density (the nuclei). The two other types occur as a consequence of particular geometrical arrangements of bond paths and define elements of molecular structure. If the bond

* To whom correspondence should be sent.
[†] Facultat de Química.
[‡] Facultat de Farmàcia.

10.1021/jp983382s CCC: $18.00
Published on Web 01/14/1999

TABLE 1: Interaction Energies (E, kcal/mol), Equilibrium Distances (R_e, Å), and Selected Electron Density Topological Properties for $Na^+-\pi$ Complexes of Benzene Derivatives, Pyridine, Naphthalene, and Indole

compound	E	R_e	CP[a]	n	$10^2\rho$	$10^2\nabla^2\rho$	r_{cp}
H	−27.1	2.45	(3, −1)	6	0.991	4.682	1.41
			(3, +1)	6	0.989	4.671	1.41
			(3, +3)	1	0.791	4.115	1.19
NH_2	−31.8	2.43	(3, −1)	1	1.094	5.225	1.41
			(3, +1)	1	0.940	4.435	1.38
			(3, +3)	1	0.816	4.221	1.17
OH	−26.9	2.46	(3, −1)	1	1.093	5.175	1.42
			(3, +1)	1	0.867	4.071	1.40
			(3, +3)	1	0.780	3.994	1.20
BH_2	−24.4	2.46	(3, −1)	1	0.974	4.595	1.42
			(3, −1)	2	0.977	4.560	1.42
			(3, +1)	1	0.953	4.468	1.41
			(3, +1)	2	0.969	4.593	1.41
			(3, +3)	1	0.777	4.024	1.20
F	−22.0	2.50	(3, −1)	1	1.019	4.735	1.45
			(3, +1)	1	0.813	3.841	1.43
			(3, +3)	1	0.733	3.739	1.23
Cl	−21.5	2.49	(3, −1)[b]	1	0.942	4.392	1.43
			(3, −1)[c]	1	0.911	4.376	1.44
			(3, +1)	2	0.911	4.375	1.43
			(3, +3)	1	0.752	3.878	1.23
1,3-diF	−16.8	2.54	(3, −1)	2	0.846	3.891	1.48
			(3, +1)	2	0.828	3.860	1.47
			(3, +3)	1	0.690	3.478	1.27
CN	−15.7	2.54	(3, −1)[b]	1	0.851	3.896	1.47
			(3, −1)[c]	1	0.840	4.067	1.47
			(3, −1)	2	0.852	3.906	1.47
			(3, +1)[d]	2	0.851	3.891	1.46
			(3, +1)[e]	2	0.837	4.008	1.46
			(3, +3)	1	0.692	3.578	1.26
1,3,5-triF	−12.4	2.60	(3, −1)	3	0.774	3.484	1.53
			(3, +1)	3	0.742	3.468	1.49
			(3, +3)	1	0.634	3.142	1.31
pyridine	−20.0	2.51	(3, −1)	2	0.915	4.191	1.46
			(3, +1)[b]	1	0.904	4.147	1.45
			(3, +1)[f]	1	0.789	4.080	1.42
			(3, +3)	1	0.714	3.882	1.25
naphthalene	−28.7	2.43	(3, −1)	2	1.041	4.854	1.42
			(3, +1)[g]	1	0.957	4.674	1.39
			(3, +1)[h]	1	1.004	4.794	1.39
			(3, +3)	1	0.794	4.105	1.18
indole	−32.6	2.41	(3, −1)	1	1.220	5.856	1.38
			(3, +1)	1	0.892	4.308	1.38
			(3, +3)	1	0.810	4.204	1.17

[a] The electron density (ρ, atomic units) and its Laplacian ($\nabla^2\rho$, atomic units) at the (3, −1), (3, +1) and (3, +3) critical points (CP) originated upon complexation are given, as well as the total number (n) of each CP in the complex and the distance (r_{cp}, Å) from the aromatic ring to the CP. [b] Near C4. [c] Near C1. [d] Near C3 (C5). [e] Near C2 (C6). [f] Near N. [g] Near C2−C3. [h] Near C9−C10.

paths are linked so as to form a ring of bonded atoms, a (3, +1) ring critical bond is formed in the interior of the ring. If the bond paths are arranged as to enclose the interior of a molecule with ring surfaces, then a (3, +3) cage critical point is found in the interior of the cage, the charge density being a local minimum at such a point.

Computational Details. Different series of cation−π complexes were considered in the study. Initially, we considered the interaction of the Na^+ cation with benzene and its fluoro, hydroxy, amino, boro, chloro, cyano, 1,4-difluoro, and 1,3,5-trifluoro derivatives, as well as pyridine, naphthalene, and indole. The choice of these compounds was motivated by two reasons: (i) they cover a variety of substituents and aromatic cores, which are expected to lead to relevant differences in the π-electron distribution with regard to the benzene molecule and (ii) previous studies have addressed the energetics of the interaction of those compounds with Na^+,[1,12,15] which facilitates examination of the relationship of the electron density topological properties with both energetic and geometrical features in these complexes. Moreover, we extended the study to the interaction of the Na^+ cation with the five-membered rings of azulene, pyrrole, furan, indole, and imidazole. Finally, the interaction of benzene with a variety of cations, including H^+, Mg^{2+}, Li^+, Na^+, and NH_4^+, and hydrogen-bonded neutral molecules, like hydrogen fluoride and methane, was also considered. This allowed us to examine the topological changes in electron density originated from the nature of both the cation and the π-electron system.

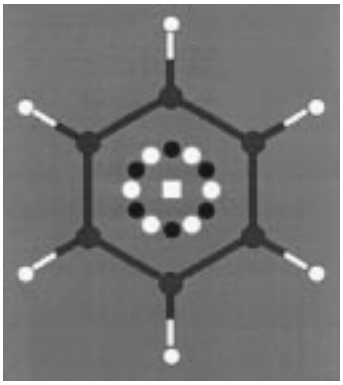

Figure 1. Schematic on-top representation of the location of the six (3, −1) (dark circles) and six (3, +1) (white circles) critical points, and of the (3, +3) (squares) critical point originated from the interaction of the Na^+ cation with benzene. The cation lies in the normal to the benzene passing through the center of the ring.

The geometry of all the complexes was fully optimized at the Hartree−Fock level using the 6-31G(d,p)[30] basis with the only exception of the complex formed between benzene and NH_4^+. In this case the minimum energy structure has two N−H hydrogens directed toward the benzene ring,[8] but we imposed one N−H hydrogen pointing toward the benzene ring in order to allow direct comparison with the rest of the complexes. Interaction energies were determined at the HF/6-31G(d,p) level, since previous studies[1,12,13] demonstrated that reliable quantitative results are obtained at this level of theory, without correction for the basis set superposition error. Indeed, we must note that neither the number nor the quality of the critical points change upon inclusion of electron correlation effects.[31,32]

Results

Table 1 reports the energies and equilibrium distances corresponding to the interaction of Na^+ with a series of benzene derivatives, as well as with pyridine and the six-membered ring of indole and naphthalene. The exploration of the critical points for the interaction of benzene with Na^+ revealed the existence of six (3, −1) critical points, which are symmetrically distributed and connect the cation with the carbon atoms (see Figure 1). The bond path follows closely the geometric line from the carbon atom to the Na^+ ion, since the difference between the bond path length and the interatomic distance is slightly less than 0.01 Å. The Laplacian of the (3, −1) critical points is positive, indicating a depletion of electron energy, as is characteristic of closed-shell interactions.[16,17] There are also six (3, +1) ring critical points, each placed along the line connecting the Na^+ cation with the middle of the C−C bond, that separate every pair of (3, −1) bond critical points (see Figure 1). There is a very small difference between the values of the electron density changes at the alternating bond and ring critical points. Finally, the interaction is further characterized by the existence

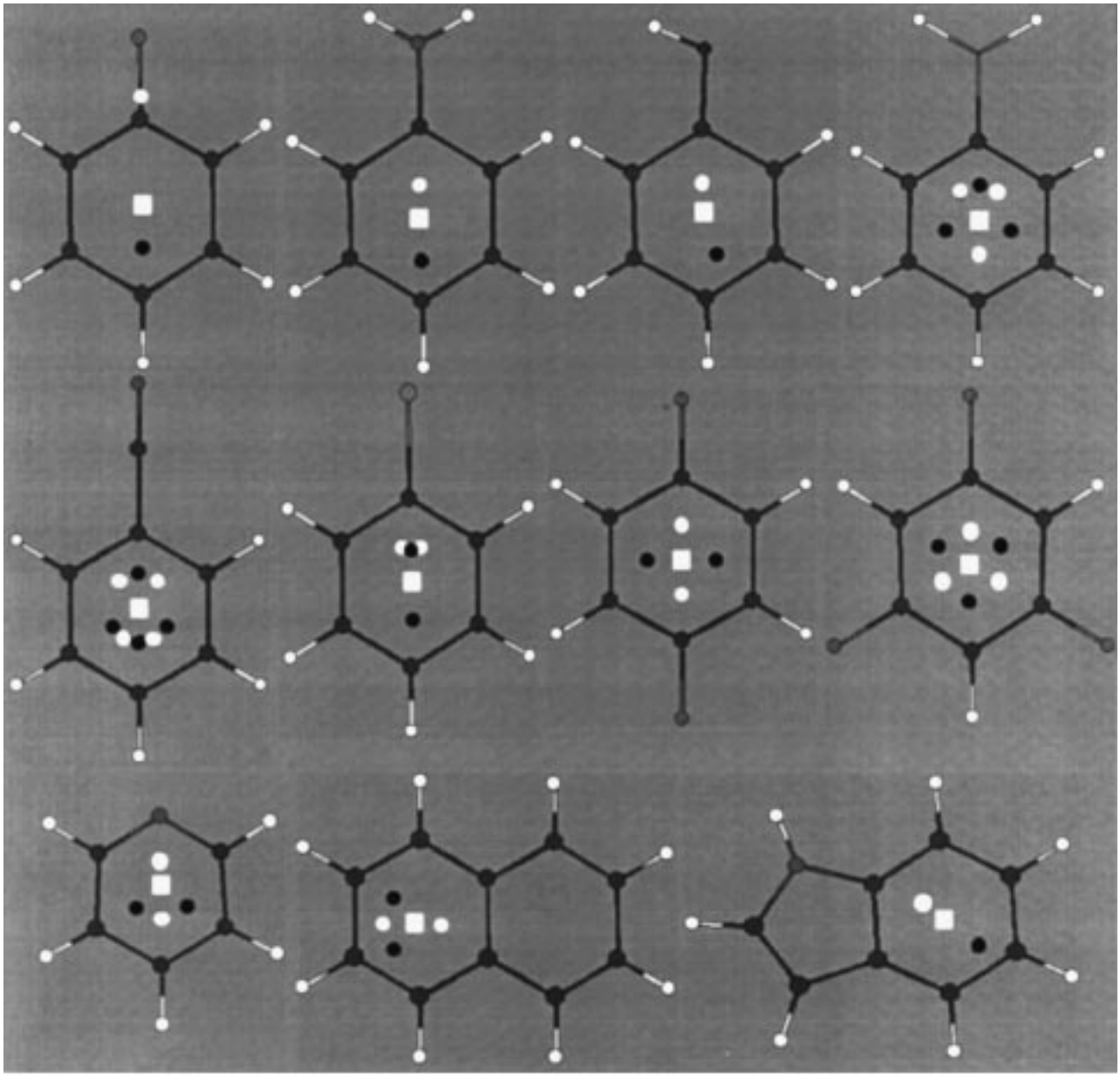

Figure 2. Schematic on-top representation of the location of the (3, −1) (dark circles), (3, +1) (white circles), and (3, +3) (squares) critical points originated from the interaction of the Na^+ cation with benzene derivatives: (top) fluoro, amino, hydroxy, boro; (middle) cyano, chloro, 1,4-difluoro, and 1,3,5-trifluoro; (bottom) pyridine, naphthalene, and the six-membered ring of indole. The cation lies in the normal to the benzene passing through the center of the ring.

of a (3, +3) cage critical point located along the line connecting the Na^+ ion with the center of the ring.

The above-mentioned pattern of critical points that appears upon complexation of the Na^+ ion with benzene is drastically altered by the introduction of substituents (see Table 1 and Figure 2). Only one (3, −1) bond critical point lying between the cation and the carbon at position 4 (para to the substituent) was found for fluorobenzene, aniline, and phenol. The attachment of $-BH_2$ and −CN groups leads to the appearance of three and four bond critical points, respectively. In the former case they connect the cation to carbon atoms C1, C3, and C5, while in the latter the bond path connects the Na^+ ion with atoms C1, C3, C4, and C5. Two bond critical points connecting the cation with atoms C1 and C4 occur in chlorobenzene. Likewise, two and three (3, −1) critical points occur for 1,4-difluoro and 1,3,5-trifluoro derivatives. In the former they are in the plane normal to the molecule passing through the middle of the C2−C3 and C5−C6 bonds, while in the latter they connect the Na^+ ion with the carbon atoms C2, C4, and C6. In the case of pyridine, two bond critical points are found in the line connecting the cation with atoms C3 and C5. Two (3, −1) critical points are found for naphthalene, which connect the cation with carbons C2 and C3. Finally, the approach of Na^+ to the six-membered ring of indole leads to the appearance of one (3, −1) critical point, which connects the cation with C6.

The variation in the number and location of the bond critical points is also reflected in the distribution of the (3, +1) critical points (see Table 1). Thus, the ring critical point in fluorobenzene, aniline, and phenol occurs near the carbon C1, the atom bearing the substituent. A similar pattern is found in chlorobenzene, even though the two symmetrical ring critical points reside very close to the (3, −1) critical point. In the derivatives boro, cyano, 1,4-difluoro, and 1,3,5-trifluoro there is a clear alternance between ring and bond critical points. The two ring critical points in pyridine are in the plane normal to the molecule passing through the line N···C4. Finally, the ring critical point

lies near the bond C9−C10 in naphthalene and the carbon vicinal to the nitrogen in indole.

The topology found in fluorobenzene, aniline, and phenol is particularly interesting. In their complexes a single (3, −1) critical point occurs along the line connecting the carbon C4 and the Na^+ ion (see above) and, in addition to the (3, +1) critical point found in the molecular plane of benzene, a single ring critical point appears near C1. This means that the surface of such a ring critical point extends from the C4−Na^+ bond path all around the ring back to the same bond path and, as a result, the topology of the electron density exhibits a cage critical point in those complexes.

The diversity in the distribution pattern of bond and ring critical points reflects the profound influence of the number and nature of substituents on the electron density of the benzene ring. Thus, the appearance of the bond critical point para to the substituent in fluorobenzene, aniline, and phenol, as well as the ring critical point near the carbon bearing the substituent, reflects the combined influence of the electron-withdrawing and resonance effects of these substituents. Likewise, the pattern found in the mono-, di-, and trifluorinated derivatives can be realized from the electron-withdrawing effect of the fluorine atom. The topological distribution in pyridine can be understood from the deactivating effect of the nitrogen, leading to the bond critical bonds at C3 and C5 and the ring ones near the nitrogen and C4 atoms. Similarly, the location of the bond critical points in naphthalene likely reflects the tendecy to maintain the resonance in the fused six-membered ring, whereas the (3, −1) critical point in indole is formed near the carbon lying in para to the one supporting the nitrogen. Indeed, the influence of the substituent is also noted in the values of the electron density at the bond and ring critical points, which exhibit differences sensibly larger than those found for the benzene−Na^+ complex, revealing more abrupt changes in the electron density distribution (see Table 1). To gain deeper insight into the role of the substituent on the pattern of bond critical points, the Laplacian of the charge density, which determines where the charge density is locally concentrated or depleted, [16,17] and the ellipticities of the phenyl C−H bonds were examined in both the isolated compounds and the complexes. These properties were chosen since they have been used to discuss the directing ability and activating−deactivating effects of a substituent in electrophilic aromatic substitution.[33] Unfortunately, no direct relationship was observed between the bond path distribution and neither the secondary concentration in the valence-shell charge concentration that is found above each of the carbon atoms[33] nor the C−H ellipticities.

The diversity in the topological pattern of the electron density precludes the possibility to relate the energetics of these complexes with the properties of the bond critical points, as has been performed for other intermolecular interactions.[20,23−26] The only common topological feature in all the complexes is the existence of the (3, +3) cage critical point. The values of the density and the Laplacian of the cage critical point, as well as their distance from the ring, are also given in Table 1. Comparison of the energy and equilibrium distances with the properties of the (3, +3) critical points reveals a number of interesting trends. Particularly, there is a strong correlation between the charge density (ρ) at the cage critical point and the interaction energy (E), as noted in the regression equation $E = (59.3-110.4) \times 10^2\rho$ ($r = 0.98$), where the energy is given in kcal/mol and the density is in atomic units (see Figure 3). Furthermore, there is a close correlation between the value of the electron density at the cage critical bond and the equilibrium distance (R_e) from the ring to the Na^+ cation, as shown by the regression equation $R_c = (3.22-0.98) \times 10^2\rho$ ($r = 0.99$), where the equilibrium distance is given in angstroms (see Figure 3). The variation in the location of the cage critical points (r_{cp}) in the complexes follows closely the change in the equilibrium distance ($R_c = 0.99-1.22r_{cp}$; $r = 0.99$; R_e and r_{cp} in angstroms). Finally, there are also strong correlations between the interaction energy ($r = 0.94$) and the equilibrium distance ($r = 0.98$) with the Laplacian of the electron density at the (3, +3) critical point. As noted in previous studies,[26,27,31] these relationships allow us to generalize the concept of bond order to $Na^+-\pi$ interactions.

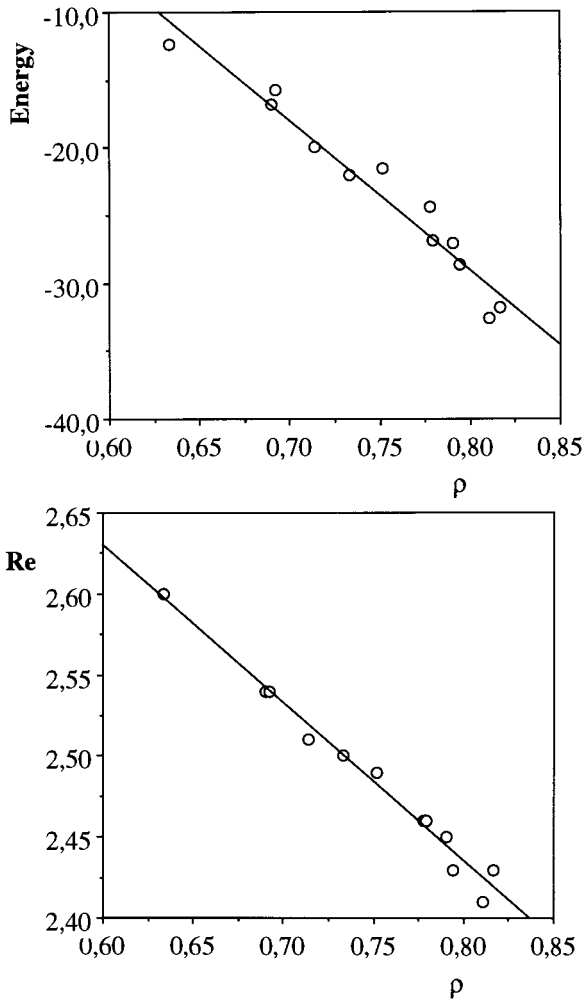

Figure 3. Plots of the regression between the electron density (a.u.) at the (3, +3) critical point and (top) the interaction energy (kcal/mol) and (bottom) the equilibrium distance (Å) for the $Na^+-\pi$ complexes in six-membered rings.

The preceding results point out the relationship between the properties of the cage critical points and the energetics and geometrical characteristics of $Na^+-\pi$ complexes in six-membered rings. This prompted us to investigate the validity of similar relationships in cation−π complexes involving five-membered rings. At this point, we examined the topological features of the electron density for the interaction of Na^+ with pyrrole, imidazole, furan, and the five-membered rings of indole and azulene.

The number and nature of critical points vary considerably between the different molecules (see Table 2 and Figure 4). In the case of pyrrole there are two (3, −1) critical points, which connect the cation with atoms C3 and C4, separated by one ring critical point. Replacement of the carbon C3 of pyrrole by nitrogen (imidazole) leads to the disappearance of one bond

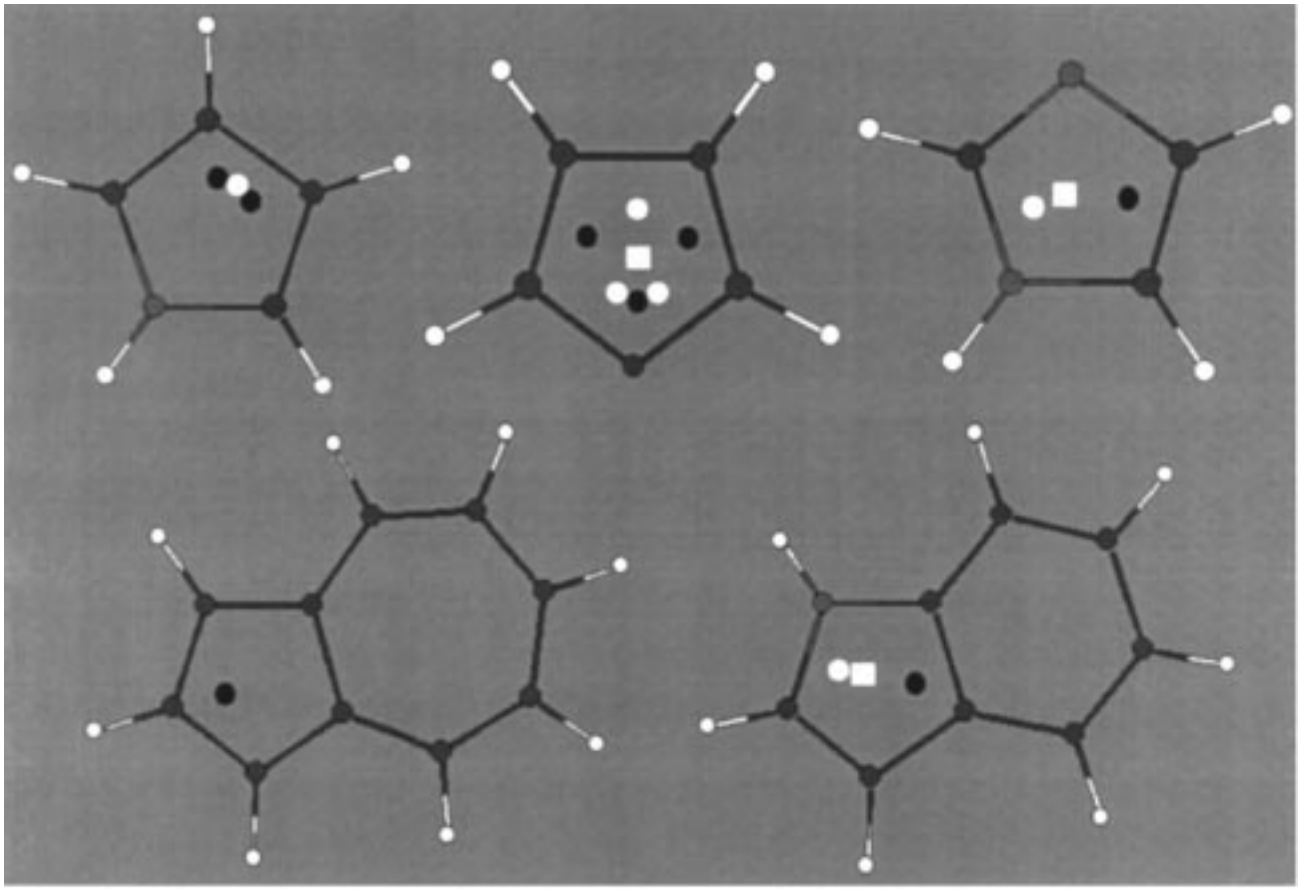

Figure 4. Schematic on-top representation of the location of the (3, −1) (dark circles), (3, +1) (white circles), and (3, +3) (squares) critical points originated from the interaction of the Na^+ cation with (top) pyrrole, furan, and imidazole and (bottom) the five-membered rings of azulene and indole. The cation lies in the normal to the benzene passing through the center of the ring.

TABLE 2: Interaction Energies (*E*, kcal/mol), Equilibrium Distances (R_e, Å), and Selected Electron Density Topological Properties for Na^+−π Complexes Involving Five-membered Rings

compound	E	R_e	CP[a]	n	$10^2\rho$	$10^2\nabla^2\rho$	r_{cp}
azulene	−34.1	2.44	(3, −1)	1	1.379	6.792	1.38
pyrrole	−29.6	2.47	(3, −1)	2	1.341	6.610	1.43
			(3, +1)	1	1.338	6.635	1.42
indole	−29.0	2.47	(3, −1)	1	1.246	6.476	1.42
			(3, +1)	1	0.941	5.684	1.34
			(3, +3)	1	0.928	5.787	1.26
furan	−21.0	2.50	(3, −1)	1	0.919	6.225	1.39
			(3, −1)	2	1.027	5.084	1.47
			(3, +1)	2	0.913	6.100	1.38
			(3, +1)	1	0.946	4.635	1.42
			(3, +3)	1	0.849	5.582	1.29
imidazole	−21.0	2.50	(3, −1)	1	1.123	5.626	1.46
			(3, +1)	1	0.894	5.627	1.40
			(3, +3)	1	0.859	5.692	1.30

[a] The electron density (ρ, atomic units) and its Laplacian ($\nabla^2\rho$, atomic units) at the (3, −1), (3, +1) and (3, +3) critical points (CP) originated upon complexation are given, as well as the total number (n) of each CP in the complex and the distance (r_{cp}, Å) from the aromatic ring to the CP.

critical point, while the bond path of the remaining (3, −1) critical point connects the cation with the atom C4. Likewise, replacement of the NH group of pyrrole by oxygen (furan) leads to three bond critical points, which connect the Na^+ ion with the oxygen and the carbon atoms C2 and C5, each pair of bond critical points being separated by a ring critical point. In the case of indole, a (3, −1) critical point connects the cation with the carbon C4, and there exists a ring critical point opposite to it between the bond N−C2. In azulene there is simply one bond critical point, whose bond path connects the cation with the carbon C10. Finally, in contrast with the topology found for the complexes involving six-membered rings, which all shared a cage critical point, this kind of critical point is found only in furan, imidazole, and indole.

Again, the nature of the heteroatom and of the fused ring largely modulates the topological pattern in complexes involving five-membered rings. Particularly, the large differences arising upon replacement of the NH group in pyrrole by the oxygen atom in furan are remarkable. Thus, whereas the bond critical points appear near C3 and C5 for the former, the reverse trend is observed for furan. This reflects the differences in resonance and electron-withdrawing effects for the groups −NH− and −O−, as noted in the ellipticities of the bond critical points for the bonds N−C2 (pyrrole) and O−C2 (furan) bonds, which amount to 0.110 and 0.019, respectively (0.152 and 0.049 for the uncomplexed molecules). It is also worth noting the effect of the six-membered ring in indole, which makes the bond critical point to appear in the position that reinforces conjugation of the nitrogen lone pair with the fused benzene ring, as compared with the two symmetrical bond critical points in pyrrole. Likewise, the differences observed between indole and azulene suggest that resonance effects are more involved in the former. In fact, it is known that in azulene the bond shared by the two rings, which has the smallest ellipticity (0.074) of all the C−C bonds, is significantly longer than the rest of bonds, indicating a predominantly single-bond character.[32]

The lack of a common topological feature to all the complexes reported in Table 2 precludes establishing relationships similar

TABLE 3: Interaction Energies (E, kcal/mol), Equilibrium Distances (R_e, Å) and Selected Electron Density Topological Properties for the Complexes of Benzene with Cations and Hydrogen-bonded Neutral Molecules

compound	E	R_e	CP[a]	$10^2\rho$	$10^2\nabla^2\rho$	r_{cp}
H^+	−121.7	1.73	(3, −1)	6.665	7.842	0.63
			(3, +1)	6.663	8.121	0.63
			(3, +3)			
Mg^{2+}	−118.8	3.76	(3, −1)	2.459	10.713	1.18
			(3, +1)	2.451	10.673	1.18
			(3, +3)	1.821	7.048	0.85
Li^+	−40.8	3.67	(3, −1)	1.418	7.673	1.24
			(3, +1)	1.415	7.670	1.24
			(3, +3)	1.161	6.308	1.03
Na^+	−27.1	4.63	(3, −1)	0.991	4.682	1.41
			(3, +1)	0.989	4.671	1.41
			(3, +3)	0.791	4.115	1.19
NH_4^+	−13.9	4.12	(3, −1)	0.973	3.374	1.38
			(3, +1)	0.972	3.377	1.57
			(3, +3)	0.812	3.621	1.16
HF	−3.5	4.72	(3, −1)	0.481	1.981	1.57
			(3, +1)	0.480	1.980	1.57
			(3, +3)	0.433	2.018	1.43
CH_4	−0.3	6.53	(3, −1)	0.122	0.487	2.02
			(3, +1)	0.121	0.487	2.02
			(3, +3)	0.114	0.526	1.92

[a] The electron density (ρ, atomic units) and its Laplacian ($\nabla^2\rho$, atomic units) at the (3, −1), (3, +1) and (3, +3) critical points (CP) originated upon complexation are given, as well as the distance (r_{cp}, Å) from the aromatic ring to the CP.

to those examined before. This behavior is in contrast to the results observed in six-membered rings. In this latter case the effect of changes such as the replacement of −CH− by −N− or the presence of fused rings seems to be better accommodated, as suggested by previous topological studies in azines.[34] In this sense, the electron density in five-membered rings appear to be sensibly more susceptible to the influence of heteroatoms than that in larger rings.

The last point examined here is the characteristics of the cation−π interactions in complexes involving other types of cations or even hydrogen-bonded neutral molecules. Table 3 reports the interaction energies and equilibrium distances for the interaction of benzene with Li^+, Na^+, NH_4^+, and Mg^{2+}, as well as with H^+ and two neutral molecules, hydrogen fluoride and methane, which were also included to examine the interaction with the hydrogen atom in hydrogen-bonded complexes. The topological pattern of critical points reported above for the interaction of benzene with the Na^+ cation is reproduced in all cases (see Figure 1) with the only exception of the interaction with H^+, where no cage critical point was detected. At this point, it must be stressed that no ring critical point was found in the molecular plane of benzene in the benzene−H^+ complex. This is necessary to satisfy the Poincaré−Hopf relationship. In fact, when one examines the profile of the electron density along the line passing through the center of the benzene ring from the H^+, it is found that the electron density decreases monotonically from the maximum value, which occurs at the position of the H^+.

Inspection of the results in Table 3 indicates that, apart from the H^+−benzene complex (see below), there is a relationship between the interaction energy and the electron density at the cage critical point ($E = (25.8-70.0) \times 10^2\rho$; $r = 0.94$). Since all the complexes exhibit the same topological pattern, such an analysis can also be extended to the bond critical points. Thus, there is also a strong correlation between the interaction energy and the electron density at the (3, −1) critical point ($E = (21.9-52.1) \times 10^2\rho$; $r = 0.96$). Moreover, such a correlation is also apparent when one considers the electron density at the (3, −1) critical points located at the C−C bonds (see Table 4), as noted in the regression equation $E = (-3651.1 + 1117.6) \times 10^2\rho$; $r = 0.99$. Similar results are obtained when the Laplacian of the electron density is considered. It is worth stressing the relevance of all these relationships, since they cover a variation of 2 orders of magnitude in the interaction energy and allow for treating simultaneously the interaction with both cations and hydrogen-bonded neutral molecules.

TABLE 4: Electron Density (ρ, Atomic Units) and Its Laplacian ($\nabla^2\rho$, Atomic Units) at the (3, −1) Critical Points Associated with the C−C Bonds in Benzene and Their Ellipticity (ϵ) for the Complexes of Benzene with Cations and Hydrogen-bonded Neutral Molecules[a]

compound	$10^2\rho$	$10^2\nabla^2\rho$	ϵ	q
H^+	3.211	−9.759	0.203	0.57
Mg^{2+}	3.166	−9.575	0.183	1.82
Li^+	3.225	−9.876	0.211	0.94
Na^+	3.236	−9.943	0.215	0.94
NH_4^+	3.251	−10.020	0.224	0.96
HF	3.268	−10.119	0.229	−0.01
CH_4	3.273	−10.161	0.230	0.00

[a] The net charge (q; units of electron) of the interacting compound is also given.

The influence of the interacting (cation or hydrogen-bonded) compound on the electron density can be followed from the ellipticity of the electron density at the (3, −1) critical points of the C−C bonds in the benzene ring. In the case of benzene, the ellipticity of the C−C bond determined from the HF/6-31G-(d,p) wave function is 0.231, which seems reasonable for a bond with an order of 1.5.[35] Table 4 lists the ellipticities determined for the (3, −1) critical points in the C−C bonds. Again, with exception of the H^+−benzene complex, there is a clear relationship between the interaction energy and the electron density deformation induced by the polarizing effect of the interacting molecule ($E = -572.5 + 2500.7\epsilon$; $r = 0.99$).

The preceding results show the generalization of the topological properties of electron density in cation−π complexes to a variety of cations and also to the interaction with the hydrogen atom in hydrogen-bonded neutral molecules. As mentioned above, the only exception to the preceding findings is the interaction of benzene with H^+. The reason for this discrepancy stems from the different nature of the proton, which yields an interaction not defined simply in terms of electrostatic and polarization effects. Thus, very recently,[15] we have shown that the GMIPp (Generalized Molecular Interaction Potential with polarization[36,37]), which evaluates the interaction energy summing up electrostatic, polarization, and van der Waals energy components, reproduces very well the SCF interaction energies for a series of 16 complexes of Na^+ with aromatic compounds. Such an agreement was possible due to the small magnitude of the charge transfer between the aromatic molecule and the cation. In fact, the charge transfer is around 0.05 units of electron for the complexes shown in Table 1 (data not shown) and similar values are found for the complexes given in Table 4. However, the charge transfer in the case of H^+ is on the order of 0.4 units of electron, and accordingly it is expected to contribute decisively to the nature of the interaction with benzene.

Conclusions

The results reported in this study demonstrate the complexity of the topology of the electron density in cation−π complexes, as noted by the variation in the nature and number of critical points. Such a diversity in the topological characteristics reflects

the profound influence exerted by the heteroatoms and substituents on the electron density. Nevertheless, the presence of the cage critical point shared by all the complexes involving six-membered rings allows us to generalize the bond order−bond length relationships reported for other kinds of intermolecular interactions. These relationships are shown to hold for the interaction of Na^+ with a variety of aromatic compounds differing in the substituents and the presence of heteroatoms or fused rings. Indeed, it is also shown that the topological pattern found for the interaction of benzene with Na^+ is applicable to other cations and even to hydrogen-bonded neutral molecules. In contrast, such relationships cannot be established for complexes involving five-membered rings, which likely stems froms a larger difficulty to accommodate the changes in electron density raised by heteroatoms and substituents.

Acknowledgment. We thank Prof. R. W. F. Bader for providing us with a copy of the PROAIM computer program. This work was supported by the DGICYT under projects PB97-0908 and PB96-1005 and by the Centre de Supercomputació de Catalunya (CESCA; Molecular Recognition Project).

References and Notes

(1) Ma, J. C.; Dougherty, D. A. *Chem. Rev.* **1997**, *97*, 1303.
(2) Sussman, J. L.; Harel, M.; Frolow, F.; Oefner, C.; Goldman, A.; Tolker, L.; Silman, I. *Science* **1991**, *253*, 872.
(3) Harel, M.; Scalk, I.; Ehret-Sabatier, L.; Bouet, F.; Goeldner, M.; Hirth, C.; Axelsen, P. H.; Silman, I.; Sussman, J. L. *Proc. Natl. Acad. Sci. U.S.A.* **1993**, *90*, 9031.
(4) Ngola, S.; Dougherty, D. A. *J. Org. Chem.* **1998**, *63*, 4566.
(5) Ting, A. Y.; Shon, I.; Lucero, C.; Schultz, P. G. *J. Am. Chem. Soc.* **1998**, *120*, 7135.
(6) Zoltewicz, J. A.; Maier, N. M.; Fabian, W. M. F. *J. Org. Chem.* **1998**, *63*, 4985.
(7) Deakyne, C. A. In: *Molecular Interactions. From van der Waals to Strongly Bound Complexes*; Scheiner, S., Ed.; Wiley: Chichester, U.K., 1997; pp 265−296.
(8) Kim, K. S.; Lee, J. Y.; Lee, S. J.; Ha, T.-K.; Kim, D. H. *J. Am. Chem. Soc.* **1994**, *116*, 7399.
(9) Lee, J. Y.; Lee, S. J.; Choi, H. S.; Cho, S. J.; Kim, K. S.; Ha, T.-K. *Chem. Phys. Lett.* **1995**, *232*, 67.
(10) Caldwell, J. W.; Kollman, P. A. *J. Am. Chem. Soc.* **1995**, *117*, 4177
(11) Basch, H.; Stevens, W. J. *J. Mol. Struct. (THEOCHEM).* **1995**, *338*, 303.
(12) Dougherty, D. A. *Science* **1996**, *271*, 163.
(13) Mecozzi, S.; West, A. P., Jr.; Dougherty, D. A. *J. Am. Chem. Soc.* **1996**, *118*, 2307.
(14) Chipot, C.; Maigret, B.; Pearlman, D. A.; Kollman, P. A. *J. Am. Chem. Soc.* **1996**, *118*, 2998.
(15) Cubero, E.; Luque, F. J.; Orozco, M. *Proc. Natl. Acad. Sci. U.S.A.* **1998**, *95*, 5976.
(16) Bader, R. F. W. *Chem. Rev.* **1991**, *91*, 893.
(17) Bader, R. F. W. *Atoms in Molecules. A Quantum Theory*; Oxford University Press: Oxford, U.K., 1990.
(18) Carroll, M. T.; Chang, C.; Bader, R. F. W. *Mol. Phys.* **1988**, *63*, 387.
(19) Tang, T.-H.; Hu, W. J.; Yan, D. Y.; Cui, Y. P. *J. Mol. Struct. (THEOCHEM)* **1990**, *207*, 319.
(20) Koch, U.; Popelier, P. *J. Phys. Chem.* **1995**, *99*, 9747.
(21) Gonzalez, L.; Mó, O.; Yañez, M.; Elguero, J. *J. Mol. Struct. (THEOCHEM)* **1996**, *371*, 1.
(22) Alkorta, I.; Rozas, I.; Elguero, J. *Theor. Chim. Acc.* **1998**, *99*, 116.
(23) Popelier, P. L. A. *J. Phys. Chem. A* **1998**, *102*, 1873.
(24) Luque, F. J.; Lopez, J. M.; de la Paz, M. L.; Vicent, C.; Orozco, M. *J. Phys. Chem. A* **1998**, *102*, 6690.
(25) Novoa, J. J.; Lafuente, P.; Mota, F. *Chem. Phys. Lett.* **1998**, *290*, 519.
(26) Boyd, R. J.; Choi., S. C. *Chem. Phys. Lett.* **1985**, *120*, 80.
(27) Boyd, R. J.; Choi., S. C. *Chem. Phys. Lett.* **1986**, *129*, 62.
(28) Alcamí, M.; Mó, O.; Yáñez, M. *J. Phys. Chem.* **1989**, *93*, 3929.
(29) Alcamí, M.; Mó, O.; de Paz, J. L. G.; Yáñez, M. *Theor. Chim. Acta* **1990**, *77*, 1.
(30) Hariharan, P. C.; Pople, J. A. *Theor. Chim. Acta* **1973**, *28*, 213.
(31) Bader, R. F. W.; Tang, T. H.; Tal, Y.; Biegler-König, F. W. *J. Am. Chem. Soc.* **1982**, *104*, 946.
(32) Hanson, A. W. *Acta Crystallogr.* **1965**, *19*, 19.
(33) Bader, R. F. W.; Chang, C. *J. Phys. Chem.* **1989**, *93*, 2946.
(34) Wiberg, K. B.; Nakaji, D.; Breneman, C. M. *J. Am. Chem. Soc.* **1989**, *111*, 4178.
(35) Bader, R. F. W.; Slee, T. S.; Cremer, D.; Kraka, E. *J. Am. Chem. Soc.* **1983**, *105*, 5061.
(36) Orozco, M.; Luque, F. J. In: *Molecular Electrostatic Potentials: Concepts and Applications*; Murray, J., Sen, K., Eds.; Elsevier: Amsterdam, Netherlands, 1996; Vol. 3, pp 181−218.
(37) Luque, F. J.; Orozco, M. *J. Comput. Chem.* **1998**, *19*, 866.